DESY 16-064

Study of HERA ep Data at Low Q^2 and Low x_{Bj} and the Need for Higher-Twist Corrections to Standard pQCD Evolution

I. Abt[a], A.M. Cooper-Sarkar[b], B. Foster[b,c,d], V. Myronenko[d], K. Wichmann[d], M. Wing[e]

[a] Max-Planck-Institut für Physik, Werner-Heisenberg-Institut, München, Germany

[b] Physics Department, University of Oxford, Oxford, U.K.

[c] Hamburg University, I. Institute of Exp. Physics, Hamburg, Germany

[d] Deutsches Elektronen Synchrotron DESY, Hamburg, Germany

[e] University College London, U.K.

Abstract

A detailed comparison of HERA data at low Bjorken-x and low four-momentum-transfer squared, Q^2, with predictions based on ln Q^2 evolution (DGLAP) in perturbative Quantum Chromo Dynamics suggests inadequacies of this framework. The standard DGLAP evolution was augmented by including an additional higher-twist term in the description of the longitudinal structure function, F_{L}. This additional term, $F_{\mathrm{L}}\ A_{\mathrm{L}}^{\mathrm{HT}}/Q^2$, improves the description of the reduced cross sections significantly. The resulting predictions for F_{L} suggest that further corrections are required for Q^2 less than about $2\,\mathrm{GeV}^2$.

1 Introduction

Analyses of HERA and other DIS data are generally performed within the perturbative regime of Quantum Chromo Dynamics (QCD), [1] i.e. with Q^2, the four-momentum-transfer squared, sufficiently above $1\,\mathrm{GeV}^2$. The HERA data extend towards Q^2 and x_{Bj} values, where x_{Bj} is the Bjorken scaling variable, where the longitudinal structure function, F_{L}, becomes significant. Previous HERA results [2,3] suggest that QCD continues to give a good description of the data down to surprisingly low values of Q^2. This gives the possibility of not only establishing the limit below which QCD no longer describes the data, but also of investigating modifications to the standard Dokshitzer–Gribov–Lipatov–Altarelli–Parisi (DGLAP) [4–8] evolution that have been proposed in the literature, for example $\ln(1/x)$ resummations, as introduced by Balitsky–Fadin–Kuraev–Lipatov [9], or saturation. The key variable is x, the fraction of the proton momentum carried by the parton, which is identical to x_{Bj} in the quark–parton model. Saturation is expected to occur when the density of gluons becomes so large that the standard increase in gluon density as x falls is flattened off by gluon–gluon interactions and recombination. Such effects can be described by non-linear evolution equations including higher-twist corrections at low x, visualised as gluon ladders with recombining gluons [10,11].

A combination of HERA reduced cross sections for ep scattering measured by the H1 and ZEUS collaborations was recently published [3] together with a QCD analysis based solely on the DGLAP formalism, which produced a set of parton distribution functions (PDFs) called HERAPDF2.0. In this analysis, it was noted that the predictions from the PDFs of HERAPDF2.0 were not able to describe the data very well below $Q^2_{\mathrm{min}} \approx 3.5\,\mathrm{GeV}^2$, both at NLO and NNLO, where Q^2_{min} is the smallest Q^2 of the data used in the fits. In particular, the turn-over of the neutral current (NC) reduced cross section at low x_{Bj} and low Q^2 due to the contribution from F_{L}, which is directly connected to the gluon PDF [12], was not well described.

The analysis called HHT presented here focuses on a simple *ansatz* to add higher-twist terms to the DGLAP-based evolution. New sets of PDFs were extracted at next-to-leading order (NLO) and next-to-next-to-leading order (NNLO). The predictions from these analyses are compared to the reduced HERA cross sections at low Q^2 and low x_{Bj}. The predictions of HHT and HERAPDF2.0 for F_{L} are compared to measurements published separately by the H1 [13] and ZEUS [14] collaborations.

2 The HERA Data and HERAPDF2.0

The HERA data on neutral current (NC) and charged current (CC) e^+p and e^-p inclusive cross sections as combined by the H1 and ZEUS collaborations [3] were used as the input to the analysis presented here. Their kinematic range spans six orders of magnitude in x_{Bj} and Q^2, but only four orders of magnitude are usable for pQCD fits, for which Q^2_{min} must be above $1\,\mathrm{GeV}^2$. The range in x_{Bj} is automatically reduced when low-Q^2 data are excluded, because, at HERA, low x_{Bj} also implies low Q^2.

The data were previously used to extract the HERAPDF2.0 [3] set of PDFs. While the description of the data by the predictions of HERAPDF2.0 is quite good, the overall χ^2/(number of degrees of freedom, ndof) values of the various fits were around 1.2 [3]. It was observed that

these values could be reduced if $Q^2_{\rm min}$ was increased from 3.5 GeV^2 to 10 GeV^2. However, this substantially worsened the predictions for the low-Q^2 and low-$x_{\rm Bj}$ regime, which were already not particularly good either at NLO or NNLO for the standard fits with $Q^2_{\rm min} = 3.5\,{\rm GeV}^2$. Neither did NNLO fits show any improvement over NLO ones. It was also observed that the quality of the fit was influenced by the order of α_s, the strong coupling constant, to which $F_{\rm L}$ was evaluated in the heavy-flavour scheme used, which, for HERAPDF2.0, was the so-called RTOPT scheme [15–17].

Most of the HERA data were taken with a centre-of-mass energy, $\sqrt{s}$, of 318 GeV. However, NC e^+p data are available also for lower $\sqrt{s}$, such that different values of the inelasticity y are accessed at the same $x_{\rm Bj}$ and Q^2, since $y = sx/Q^2$. This provides direct information on $F_{\rm L}$ because the reduced NC cross section at low Q^2, where only photon exchange is important, can simply be written as

$$\sigma^{\pm}_{r,{\rm NC}} = F_2 - \frac{y^2}{Y_+} F_{\rm L} \,, \tag{1}$$

where $Y_+ = 1+(1-y)^2$. Although results on $F_{\rm L}$ were published separately by the H1 and ZEUS collaborations, the data on which the results were based were combined and were included in the data set used for the HHT analysis.

3 QCD Analysis Including Higher-Twist Effects

The introduction of higher-twist terms is one possible way to extend the DGLAP framework. The leading-twist perturbative QCD forms of the structure functions F_2 and $F_{\rm L}$ were augmented by a simple twist-4 term

$$F_2^{\rm HT} = F_2^{\rm DGLAP} \quad (1 + A_2^{\rm HT}/Q^2) \,, \tag{2}$$
$$F_{\rm L}^{\rm HT} = F_{\rm L}^{\rm DGLAP} \quad (1 + A_{\rm L}^{\rm HT}/Q^2) \,, \tag{3}$$

where $A_2^{\rm HT}$ and $A_{\rm L}^{\rm HT}$ are free parameters in the fits.

The ZEUSfitter package [1] was used for the analysis presented here. The results were cross-checked with the HERAFitter [19] package. Except for the addition of the higher-twist term, the fits called HHT were set up exactly as the HERAPDF2.0 fits with $Q^2_{\rm min} = 3.5\,{\rm GeV}^2$. The value of $Q^2_{\rm min} = 3.5\,{\rm GeV}^2$ was chosen as it was assumed that non-perturbative and higher-twist effects would only appear at Q^2 below this value. Other groups work with even lower $Q^2_{\rm min}$, for example MSTW/MMHT [20,21] use $Q^2_{\rm min} = 2.0\,{\rm GeV}^2$. A higher-twist term as introduced in Eq. 3 was tested by MMHT and found to improve the χ^2 values of their fits [22] to HERA and other data.

The PDFs for HHT were parameterised at the starting scale $\mu^2_{f_0} = 1.9\,{\rm GeV}^2$. The gluon PDF, directly connected to $F_{\rm L}^{\rm DGLAP}$, was parameterised as

$$xg(x) = A_g x^{B_g}(1-x)^{C_g} - A'_g x^{B'_g}(1-x)^{C'_g} \,, \tag{4}$$

where A_g, B_g, C_g and A'_g, B'_g are free parameters and C'_g was set to 25 [20]. The A'_g was added to make the parametersiation more flexible at low x. It could lead to a negative gluon density at

[1] The package was recently also used in a combined electroweak and QCD analysis of HERA data [18].

low x, even at scales above $\mu_{f_0}^2$. However, this was neither observed for HERAPDF2.0 nor for the analysis presented here.

The HHT fits were performed at NNLO and NLO, including the higher-twist term for F_2 only, F_L only and both F_2 and F_L. The uncertainties from the fits are taken as experimental uncertainties and are the only uncertainties considered throughout the paper. The introduction of A_L^{HT} was found to reduce the χ^2/ndof of the fit significantly, both at NLO and at NNLO. However, adding A_2^{HT} had no significant effect. For the NNLO fit, it only reduced the χ^2/ndof from 1363/1131 to 1357/1130 and the corresponding value of A_2^{HT} was consistent with zero, i.e. $A_2^{HT} = 0.12 \pm 0.07\,\text{GeV}^2$. Similar values for A_2^{HT} were obtained when A_2^{HT} and A_L^{HT} were included simultaneously. Therefore, all HHT fits presented in this paper include only the A_L^{HT} term. This agrees with predictions [10] that higher-twist terms would be observable in F_L but not in F_2 because the contributions from longitudinally and transversely polarised photons would cancel for F_2.

The HHT PDFs, xd_v and xu_v for the valence quarks and xS for the sea quarks together with xg, are shown in Fig. 1. The PDFs of HHT are very similar to the PDFs of HERAPDF2.0, even though the values of A_L^{HT} extracted are quite high: $A_L^{HT} = 5.5 \pm 0.6\,\text{GeV}^2$ from the NNLO and $A_L^{HT} = 4.2 \pm 0.7\,\text{GeV}^2$ from the NLO fit. In particular, the HHT NNLO fit also requires a substantial A'_g term even in the presence of the large higher-twist term. The gluon distribution thus exhibits a stronger turn-over at low x and Q^2.

The χ^2/ndof for HHT NNLO is 1316/1130 and for HHT NLO 1329/1130. This may be compared to the HERAPDF2.0 χ^2/ndof values of 1363/1131 for the NNLO and 1356/1131 for the NLO fit. This represents an improvement of $\Delta\chi^2 = -27$ for NLO and an even more significant $\Delta\chi^2 = -47$ at NNLO. Table 1 details the main contributions to this reduction of χ^2. The HHT fit at NNLO has a lower χ^2 than the fit at NLO. This is a reversal of the situation for HERAPDF2.0. Table 1 also lists the partial χ^2/ndp values for the high-precision NC e^+p data with $\sqrt{s} = 318\,\text{GeV}^2$. In addition, the χ^2/ndp values for the data points below $Q^2_{\text{min}} = 3.5\,\text{GeV}^2$ down to $2.0\,\text{GeV}^2$ are listed. These χ^2 values provide an evaluation of the quality of the predictions below Q^2_{min} and quantify that the extrapolation of HHT NNLO describes these data better than the extrapolation of HERAPDF2.0, while the description at NLO does not improve.

The AG parameterisation was also tested. It ensures that the gluon distribution is always positive definite for $Q^2 \geq \mu_{f_0}^2$. This condition has little effect at NLO. In contrast, the AG parameterisation at NNLO results in much higher χ^2/ndof values, 1389/1131 for HERAPDF2.0 and 1350/1130 for HHT. At NNLO the data favour a strong gluon turn-over whereas AG, by construction, does not allow this. The AG parameterisation is clearly not suited for fits at NNLO.

The validity of the assumption that perturbation theory is applicable in the kinematic regime of the fits is tested by the dependence of the quality of the fits, as represented by χ^2/ndof, on the value of Q^2_{min}. The value of χ^2/ndof should ideally not depend strongly on Q^2_{min}. The dependence of χ^2/ndof on Q^2_{min} for HHT and HERAPDF2.0 is shown in Fig. 2 for both NNLO and NLO. The values drop steadily until $Q^2_{\text{min}} \approx 10\,\text{GeV}^2$, when the χ^2/ndof becomes similar for HHT and HERAPDF2.0. The effect of the higher-twist term is, as expected, confined to the low-Q^2 region. The HHT fits show a slower rise in χ^2 as Q^2_{min} is reduced.

The fits with $Q^2_{\rm min} = 2.0\,{\rm GeV}^2$ close to the starting scale $\mu^2_{\rm f_0} = 1.9\,{\rm GeV}^2$ were studied in more detail. The relevant χ^2 values are listed in Table 2. The PDF and especially the higher-twist parameters of HHT NNLO do not change much when $Q^2_{\rm min}$ is lowered from $3.5\,{\rm GeV}^2$ to $2.0\,{\rm GeV}^2$. The partial χ^2/ndp for the NC e^+p data with $\sqrt{s} = 318\,{\rm GeV}$ increases from 1.12 to 1.14, but the partial χ^2/ndp drops from 1.28 to 1.04 for the 25 points in the range $2.0 \leq Q^2 < 3.5\,{\rm GeV}^2$.

Refitting with lower $Q^2_{\rm min}$ has a stronger effect at NLO than at NNLO, but again, the higher-twist term is basically unchanged. The results at NLO are as before not strongly dependent on the details of the gluon distribution. This can be seen when refitting with HHT NLO AG, which yields almost the same result as HHT NLO.

4 Heavy-Flavour Schemes

The influence of the heavy-flavour scheme was already discussed in the context of HERAPDF2.0 [3]. To study the effect on this analysis, the HERAFitter [19] package was used to replace the default RTOPT scheme with the FONLL scheme [23,24]. The resulting dependence of χ^2 on $Q^2_{\rm min}$ is shown in Fig. 3, together with the values from the standard fits.

In the FONLL scheme, the HHT NNLO fit has a substantially improved χ^2/ndof for low $Q^2_{\rm min}$ compared to HERAPDF2.0, just as for the standard HHT NNLO fit with RTOPT. The value of the higher-twist parameter $A_{\rm L}^{\rm HT} = 6.0 \pm 0.7\,{\rm GeV}^2$ is also similar. However, the HHT NLO FONLL fit has only a marginally improved χ^2/ndof for low Q^2 as compared to HERAPDF2.0 and a small value of $A_{\rm L}^{\rm HT}$, i.e. $A_{\rm L}^{\rm HT} = 1.2 \pm 0.6\,{\rm GeV}^2$. This is probably associated with the order of α_s at which $F_{\rm L}$ is evaluated. Only calculating $F_{\rm L}$ to $O(\alpha_s)$ results in a relatively large F_L, which can reduce the need for a higher-twist term. However, as soon as $F_{\rm L}$ is calculated to $O(\alpha_s^2)$ or higher, a higher-twist term is required. The best fit achieved for HHT NNLO is with the RTOPT scheme.

5 Reduced Cross Sections

A comparison of the predictions of HHT and HERAPDF2.0 with $Q^2_{\rm min} = 3.5\,{\rm GeV}^2$ to the measured reduced NC e^+p cross sections is shown at NNLO in Fig. 4 and at NLO in Fig. 5. In all cases, the predictions are extrapolated down to $Q^2 = 2.0\,{\rm GeV}^2$; HHT clearly describes this low-Q^2, low-$x_{\rm Bj}$ data better. This was already indicated by the χ^2/ndof values in Table 1, where the χ^2/ndp for the data points with $2.0 \leq Q^2 < 3.5\,{\rm GeV}^2$ are listed separately. The HHT NNLO predictions are clearly preferred as they describe the turn-over of the data towards low $x_{\rm Bj}$ quite well. This turn-over region at low $x_{\rm Bj}$ is not well described by the predictions from HERAPDF2.0.

The predictions of the HHT NNLO and HHT NLO with $Q^2_{\rm min} = 2.0\,{\rm GeV}^2$ are shown in Fig. 6. The data are well described at NNLO, even better than for the standard HHT NNLO with $Q^2_{\rm min} = 3.5\,{\rm GeV}^2$. The effect of the lower $Q^2_{\rm min}$ is stronger at NLO, where the turn-over is better described.

The HHT NNLO predictions even describe the data down to $Q^2 = 1.2\,\mathrm{GeV}^2$ quite well as can be seen in Fig. 7. This is especially true for HHT NNLO with $Q^2_{\mathrm{min}} = 2.0\,\mathrm{GeV}^2$. At $Q^2 = 1.5\,\mathrm{GeV}^2$, the turn-over is very well described. At $Q^2 = 1.2\,\mathrm{GeV}^2$, the predicted turn-over is somewhat shifted towards higher x_{Bj}. However, it is remarkable how well these data below the starting scale of the evolution are described, illustrating once again the apparent ability of a perturbative QCD *ansatz* to describe the data to surprisingly low Q^2.

6 The Structure Functions F_2 and F_{L}

Values of the structure function F_2 are extracted from the data as

$$F_2^{\mathrm{extracted}} = F_2^{\mathrm{predicted}} \frac{\sigma_r^{\mathrm{measured}}}{\sigma_r^{\mathrm{predicted}}} \quad . \tag{5}$$

The values of $F_2^{\mathrm{extracted}}$ together with $F_2^{\mathrm{predicted}}$ are shown in Figs. 8 and 9 for HHT and HERAPDF2.0 at NNLO and NLO, respectively. At NNLO, the HHT predictions and extractions agree well down to $Q^2 = 2.0\,\mathrm{GeV}^2$. Since $A_{\mathrm{L}}^{\mathrm{HT}}$ is substantial, the predictions from HHT for F_{L} are larger than from HERAPDF2.0 at low Q^2. Since $\sigma_r = F_2 - F_{\mathrm{L}}\, y^2/Y_+$, see Eq. 1, this results also in larger predictions for F_2 and in larger values of $F_2^{\mathrm{extracted}}$. The agreement between prediction and extraction is better for HHT. This suggests that the F_{L} from HERAPDF2.0 is not large enough. Also at NLO, the predicted and the extracted values agree better for HHT, even though the NLO fit is not as good as the NNLO fit below around $Q^2 = 4.5\,\mathrm{GeV}^2$.

In Fig. 10, $F_2^{\mathrm{predicted}}$ and $F_2^{\mathrm{extracted}}$ are shown for HHT NNLO and NLO with $Q^2_{\mathrm{min}} = 2.0\,\mathrm{GeV}^2$. The situation for the NNLO fit looks very similar to the fit with $Q^2_{\mathrm{min}} = 3.5\,\mathrm{GeV}^2$. The description of the data by the predictions of the NLO fit is improved at low x_{Bj} and low Q^2. However, $F_2^{\mathrm{extracted}}$ still shows a turn-over. This confirms the findings of the comparisons with the reduced cross-section data that HHT NNLO is better suited to describe the data than HHT NLO.

The H1 and ZEUS collaborations published separate measurements of F_{L} [13,14], for which data with lowered $\sqrt{s}$ provided cross sections at different y for identical x_{Bj} and Q^2. The predictions of HHT and HERAPDF2.0 with $Q^2_{\mathrm{min}} = 3.5\,\mathrm{GeV}^2$ for F_{L} at NNLO and NLO are compared to these measurements in Fig. 11. For $Q^2 > Q^2_{\mathrm{min}}$, the shapes of all predicted curves are similar but the predictions of HHT are significantly higher than those from HERAPDF2.0 for Q^2 below $50\,\mathrm{GeV}^2$. Even though the statistical accuracy of the data is limited, the data mildly favour HHT over HERAPDF2.0 in this regime.

In Fig. 11, extrapolated F_{L} predictions are shown below $Q^2_{\mathrm{min}} = 3.5\,\mathrm{GeV}^2$ and even below the starting scale $\mu^2_{\mathrm{f}_0} = 1.9\,\mathrm{GeV}^2$. These predictions have large uncertainties and the accuracy of the data is limited, but it is clear that the upturn of F_{L} predicted by HHT NNLO is not favoured by the data. This disagreement on F_{L} is in contrast to the fact that the predictions of HHT NNLO describe the very precise NC e^+p cross sections down to $Q^2 = 1.2\,\mathrm{GeV}^2$ remarkably well, see Fig. 7. Although the higher-twist term is expected to be important for F_L [10], the very large increase of the predicted F_{L} suggests that some other effect is being absorbed in F_{L} in the simple *ansatz* used in the current analysis.

Interestingly, HERAPDF2.0 NNLO also predicts a slight upturn of F_{L} at Q^2 below Q^2_{min}. This is connected to the NNLO coefficient functions, which are large and positive. Similar effects were observed previously [25] for predictions from both pure DGLAP analyses and those including higher-twist terms.

7 Saturation

The operator-product expansion beyond leading twist has diagrams in which two, three or four gluons may be exchanged in the t-channel such that these gluons may be viewed as recombining. This recombination could lead to gluon saturation [11]. The A_L^{HT}/Q^2-term used in the analysis presented here corresponds to twist-4. Another approach to describe saturation is the colour-dipole picture, which is formulated in the proton rest frame where the incoming photon develops structure over a coherence length proportional to $1/Q^2$ and $1/x_{Bj}$. Recently, fits to the HERA data were presented [26], which indicate that saturation effects should set in at latest at $x_{Bj} > 10^{-9}$, but possibly earlier. The data presented here reach down to $x_{Bj} \approx 10^{-5}$. It is therefore interesting to see if there is any hint of saturation effects becoming important already in these HERA data.

The colour-dipole framework also inspired a phenomenological model of saturation [27], Golec-Biernat–Wüsthoff (GBW), in which the onset of saturation is characterised as the transition from a "soft" to a "hard" scattering regime. This occurs along a "critical line" in the x_{Bj}, Q^2 plane. Fits to early HERA data with low Q^2 and low x_{Bj} indicated that the criticial line would be around $x_{Bj} = 10^{-4}$ at $Q^2 = 1\,\text{GeV}^2$ and $x_{Bj} = 10^{-5}$ at $Q^2 = 2\,\text{GeV}^2$ [27]. These very low-Q^2 and low-x_{Bj} data are mostly not included in the present HHT analysis. This analysis is based on the DGLAP formalism which is not expected to work for Q^2 as low as $1\,\text{GeV}^2$. The necessary Q^2_{min} cut limits the range of the fitted data in x_{Bj} such that the data used here just touch the predicted critical line.

Results on F_2 and F_L are presented for selected values of the energy at the photon–proton vertex, W, to separate out the low-x_{Bj} regime of the data ($x_{Bj} = Q^2/(W^2+Q^2)$) and to compare to the predictions of GBW. Figures 12 and 13 show extractions [2] together with the corresponding predictions for F_2 and F_L for the high-precision NC e^+p data for HHT and HERAPDF2.0 at NNLO and NLO, respectively. The data used here are limited to $Q^2 \geq Q^2_{min} = 3.5\,\text{GeV}^2$ and approach the critical regime of x_{Bj} only for $W = 276\,\text{GeV}$. The predictions of GBW, also shown in Figs. 12 and 13, agree reasonably well with the F_2 predictions of HHT up to Q^2 of about $10\,\text{GeV}^2$ at this highest W value, the only W value where HHT and HERAPDF2.0 differ significantly. The values of $F_2^{extracted}$ are significantly larger for HHT in this low-x_{Bj} regime than for HERAPDF2.0 and they agree better with the corresponding predictions. This is true for fits at NNLO and at NLO. In both cases, it is caused by significantly larger values of F_L, since Eq. 1 implies that F_2 must also increase.

For Figs. 12 and 13, all predictions from HHT and HERAPDF2.0 were extrapolated down to $Q^2 = 1.2\,\text{GeV}^2$, a value below the starting scale, for which the predictions of HHT NNLO nevertheless still describe the reduced cross sections quite well, see Fig. 7. The predictions from GBW are expected to be particularly relevant in this regime while the pQCD evolution on which HHT and HERAPDF2.0 are based is expected to start to break down. This is demonstrated by the results on F_L. The extractions and predictions differ substantially between NNLO and NLO for Q^2 below $10\,\text{GeV}^2$. At NLO, the predicted F_L values become negative for all three W values as Q^2 approaches $1\,\text{GeV}^2$ for both HERAPDF2.0 and HHT. This is unphysical. At NNLO, all predicted F_L values start to increase as Q^2 approaches $1\,\text{GeV}^2$. For HHT NNLO, this increase is dramatic.

[2] Extracted values $F_L^{extracted}$ are calculated similarly to the values of $F_2^{extracted}$, see Eq. 5.

Figures 12 and 13 also demonstrate that values of $F_L^{\text{extracted}}$ cannot be considered measurements. Even though the predictions of HHT and HERAPDF2.0 differ significantly below $100\,\text{GeV}^2$, the extractions seem to simply reflect those predictions. This demonstrates the importantance of direct F_L measurements.

Figure 14 shows predictions for F_L from HHT and HERAPDF2.0 at both NNLO and NLO for $W = 232\,\text{GeV}$ together with a prediction from GBW. The plot also contains measured values down to Q^2 of almost $1\,\text{GeV}^2$ published by the H1 collaboration [13]. The statistical accuracy of these data is limited, but the strong upturn of F_L predicted by HHT NNLO is not observed. The data confirm the downward trend of the F_L values measured for the full W range shown in Fig. 11. Colour-dipole motivated models [25,27] predict that F_L becomes similar for different values of W at low Q^2. The measured values of F_L shown in Figs. 11 and 14 are compatible with this.

The strong difference between F_L predictions from HHT NNLO and NLO, together with the HHT NNLO prediction of a strong upturn of F_L as Q^2 approaches $1\,\text{GeV}^2$ indicate that the current simple higher-twist correction to the perturbative DGLAP evolution alone cannot completely describe the physics involved, even though the reduced cross sections are described quite well by this *ansatz*.

8 Conclusions

The addition of a twist-4 term to the description of the longitudinal structure function F_L significantly improved the quality of pQCD fits within the DGLAP framework to HERA data. In particular, the description of cross sections at low Q^2 and low x_{Bj} was improved. The Q^2 range of the fits was extended down to $Q^2 = 2.0\,\text{GeV}^2$ and the cross-section data could be well described down to $Q^2 = 1.2\,\text{GeV}^2$ by extrapolations. The addition of a higher-twist term to the structure function F_2 has no effect. This confirms the expectation that the influence of higher-twist effects cancels for longitudinally and transversely polarised photons in F_2.

The recombination of gluons is part of the higher-twist formalism. This can be seen as a mechanism of saturation. The strong influence of such a higher-twist term can be seen as the first hint for the onset of saturation in the HERA data at low Q^2 and low x_{Bj}. The predictions of HHT NNLO for F_L become very high for Q^2 below $3.5\,\text{GeV}^2$ and disagree with the data. This indicates that the pQCD description is breaking down and further mechanisms are needed for a consistent description of the data at the lowest x_{Bj} and Q^2.

9 Acknowledgements

We are grateful to our ZEUS colleagues who supported this work. We thank our funding agencies, especially the Humboldt foundation, for financial support and DESY for the hospitality extended to the non-DESY authors. We also thank K. Golec-Biernat for discussions and providing the predictions of the GBW model.

References

[1] A. M. Cooper-Sarkar and R. Devenish, *Deep Inelastic Scattering* (Oxford University Press, (2011)).

[2] F. Aaron *et al.* [ZEUS and H1 Collaboration], JHEP **1001**, 109 (2010), [arXiv:0911.0884].

[3] H. Abramovicz *et al.* [ZEUS and H1 Collaboration], Eur. Phys. J. C **75**, 580 (2015), [arXiv:1506.06042].

[4] V. Gribov and L. Lipatov, Sov. J. Nucl. Phys. **15**, 438 (1972).

[5] V. Gribov and L. Lipatov, Sov. J. Nucl. Phys. **15**, 675 (1972).

[6] L. Lipatov, Sov. J. Nucl. Phys. **20**, 94 (1975).

[7] Y. Dokshitzer, Sov. Phys. JETP **46**, 641 (1977).

[8] G. Altarelli and G. Parisi, Nucl. Phys. B **126**, 298 (1977).

[9] E. Kuraev, L. Lipatov, and F. Fadin, Sov. Phys. JETP **45**, 199 (1977).

[10] J. Bartels, K. Golec-Biernat, and K. Peter, Eur. Phys. J. C **71**, 121 (2000), [hep-ph/0003042v4].

[11] J. Bartels, K. Golec-Biernat, and H. Kowalski, Phys. Rev. D **66**, 014001 (2002), [hep-ph/0203258].

[12] A. M. Cooper-Sarkar *et al.*, Z. Phys. C **39**, 281 (1988).

[13] V. Andreev *et al.* [H1 Collaboration], Eur. Phys. J. C **73**, 2814 (2013), [arXiv:1312.4821].

[14] H. Abramowicz *et al.* [ZEUS Collaboration], Phys. Rev. D **90**, 072002 (2014), [arXiv:1404.6376].

[15] R. S. Thorne and R. G. Roberts, Phys. Rev. D **57**, 6871 (1998), [hep-ph/9709442].

[16] R. S. Thorne, Phys. Rev. D **73**, 054019 (2006), [hep-ph/0601245].

[17] R. S. Thorne, Phys. Rev. D **86**, 074017 (2012), [arXiv:1201.6180].

[18] H. Abramovicz *et al.* [ZEUS Collaboration] (2016), accepted by Phys. Rev. D, [arXiv:1603.09628].

[19] S. Alekhin *et al.* (2014), [arXiv:1410.4412].

[20] A. D. Martin, W. J. Stirling, R. S. Thorne, and G. Watt, Eur. Phys. J. C **63**, 189 (2009), [arXiv:0901.0002].

[21] L. A. Harland-Lang, A. D. Martin, P. Motylinski, and R. S. Thorne, Eur. Phys. J. C **75** (2015), [arXiv:1412.3989].

[22] L. A. Harland-Lang, A. D. Martin, P. Motylinski, and R. S. Thorne (2016), [arXiv:1601.03413].

[23] M. Cacciari, M. Greco, and P. Nason, JHEP **9805**, 007 (1998), [hep-ph/9803400].

[24] S. Forte, E. Laenen, P. Nason, and J. Rojo, Nucl. Phys. B **834**, 116 (2010), [arXiv:1001.2312].

[25] A. D. Martin, W. J. Stirling, and R. S. Thorne, Phys. Lett. B **635**, 305 (2006), [hep-ph/0601247].

[26] A. Caldwell (2016), [arXiv:1601.04472v1].

[27] K. Golec-Biernat and M. Wüsthoff, Phys. Rev. D **59**, 014017 (1998), [hep-ph/9807513].

Fit at	with $Q^2_{\rm min} = 3.5\,{\rm GeV}^2$	HERAPDF2.0	HHT	$A_{\rm L}^{\rm HT}/{\rm GeV}^2$
NNLO	χ^2/ndof	1363/1131	1316/1130	5.5±0.6
	χ^2/ndp for NC e^+p: $Q^2 \geq Q^2_{\rm min}$	451/377	422/377	
	χ^2/ndp for NC e^+p: $2.0\,{\rm GeV}^2 \leq Q^2 < Q^2_{\rm min}$	41/25	32/25	
NLO	χ^2/ndof	1356/1131	1329/1130	4.2±0.7
	χ^2/ndp for NC e^+p: $Q^2 \geq Q^2_{\rm min}$	447/377	431/377	
	χ^2/ndp for NC e^+p: $2.0\,{\rm GeV}^2 \leq Q^2 < Q^2_{\rm min}$	46/25	46/25	

Table 1: Table of χ^2 values for the HHT fit compared to the equivalent HERAPDF2.0 fit, both with $Q^2_{\rm min} = 3.5\,{\rm GeV}^2$. Also listed are the partial χ^2/(number of data points, ndp) values of the fits for the high-precision NC e^+p data at $\sqrt{s} = 318\,{\rm GeV}$ for $Q^2 \geq Q^2_{\rm min}$. The final row for each fit lists the χ^2/ndp for its predictions for Q^2 below the fitted region down to $2.0\,{\rm GeV}^2$. In addition, the higher-twist parameters for HHT fits are given.

Fit at	with $Q^2_{\rm min} = 2.0\,{\rm GeV}^2$	HERAPDF2.0	HHT	$A_{\rm L}^{\rm HT}/{\rm GeV}^2$
NNLO	χ^2/ndof	1437/1171	1381/1170	5.2±0.7
	χ^2/ndp for NC e^+p: $Q^2 \geq Q^2_{\rm min}$	486/402	457/402	
	χ^2/ndp NC e^+p: $Q^2_{\rm min} \leq Q^2 < 3.5\,{\rm GeV}^2$	31/25	26/25	
NLO	χ^2/ndof	1433/1171	1398/1170	4.0±0.6
	χ^2/ndp for NC e^+p: $Q^2 \geq Q^2_{\rm min}$	487/402	466/402	
	χ^2/ndp NC e^+p: $Q^2_{\rm min} \leq Q^2 < 3.5\,{\rm GeV}^2$	40/25	31/25	

Table 2: Table of χ^2 values for the HHT fit compared to the equivalent HERAPDF2.0 fit, both with $Q^2_{\rm min} = 2.0\,{\rm GeV}^2$. Also listed are the partial χ^2/ndp values of the fits for the high-precision NC e^+p data at $\sqrt{s} = 318\,{\rm GeV}$ for $Q^2 \geq Q^2_{\rm min}$. The final row for each fit lists the partial χ^2/ndp of the fit for data points with $2.0 \leq Q^2 < 3.5\,{\rm GeV}^2$. In addition, the higher-twist parameters for HHT fits are given.

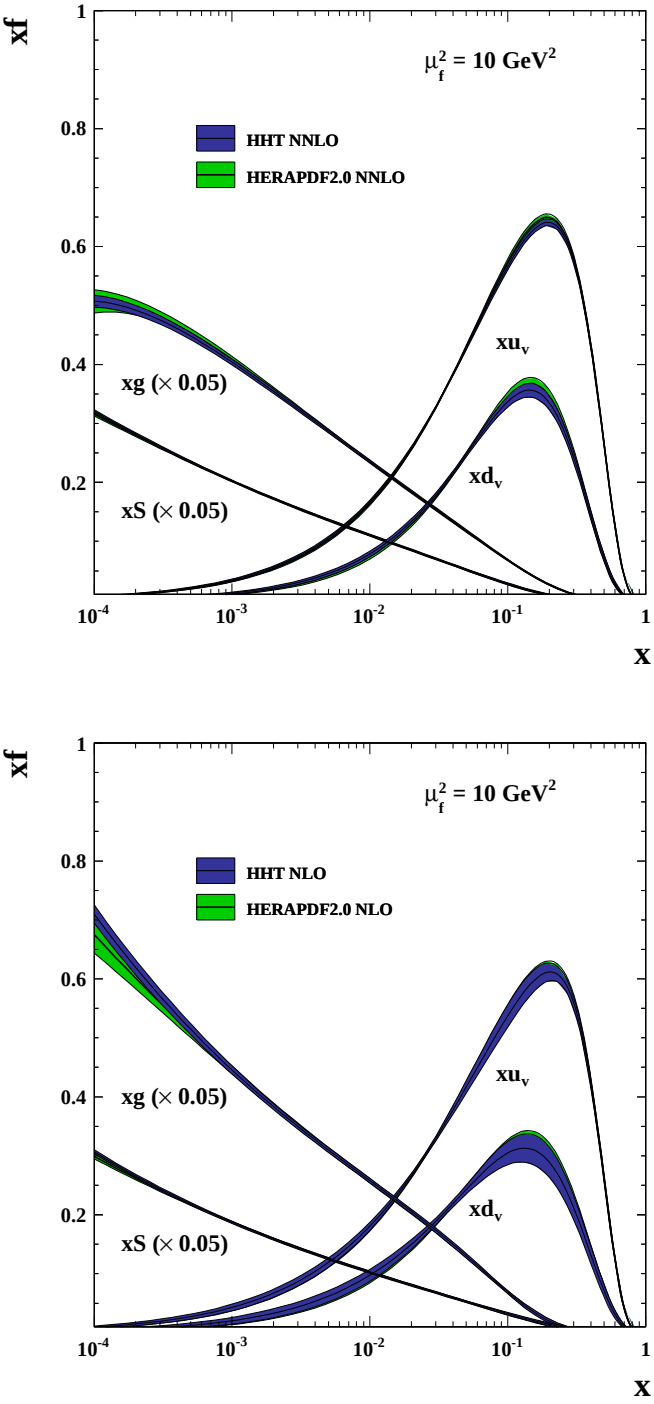

Figure 1: The HHT parton distribution functions, xu_v, xd_v, xS and xg, at the scale $\mu_f^2 = 10\,\mathrm{GeV}^2$ compared to the PDFs from HERAPDF2.0 at NNLO (top) and NLO (bottom). The gluon and sea distributions are scaled down by a factor 20. The bands represent the experimental, i.e. fit, uncertainties.

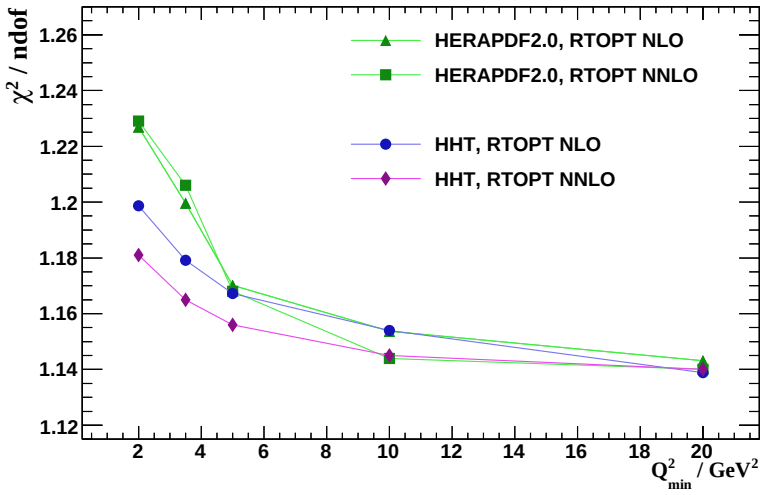

Figure 2: The χ^2/ndof versus Q^2_{min} for HHT and HERAPDF2.0 fits at NNLO and NLO.

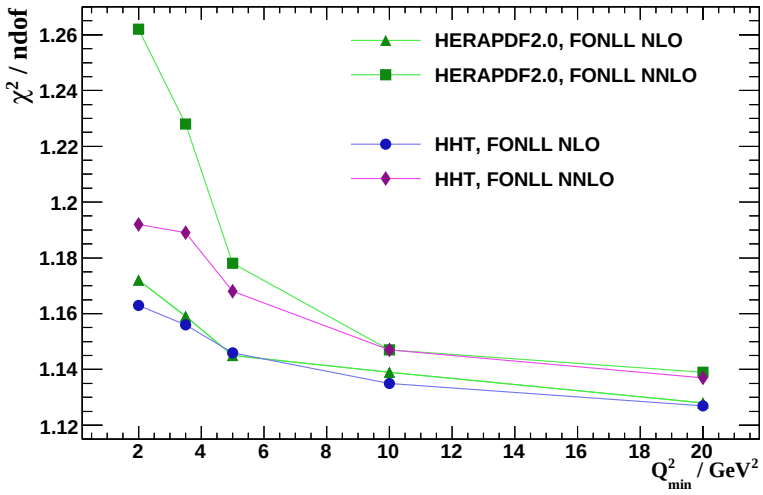

Figure 3: The χ^2/ndof versus Q^2_{min} for HHT and HERAPDF2.0 fits at NNLO and NLO using the FONLL heavy-flavour scheme instead of the default RTOPT scheme.

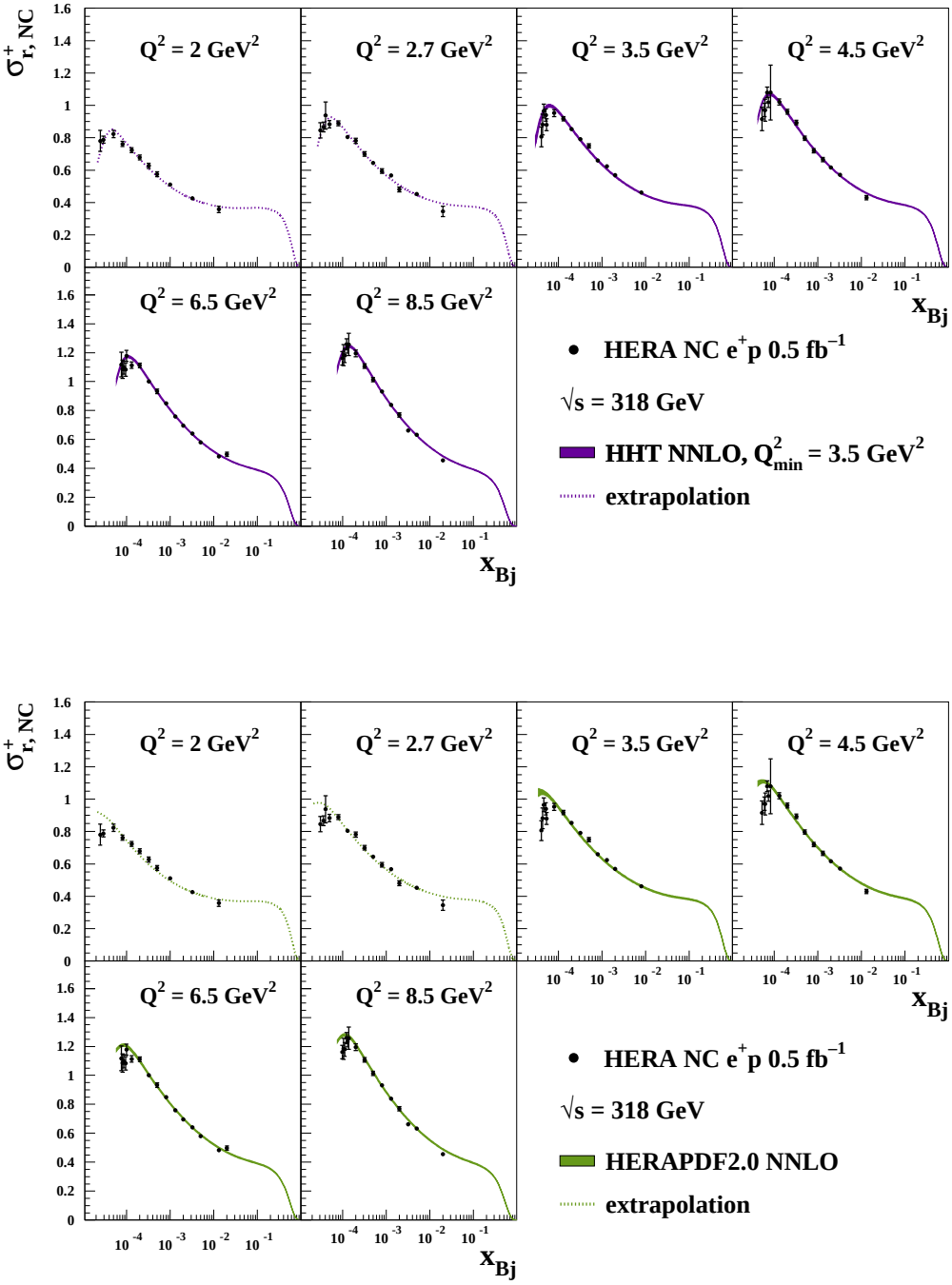

Figure 4: The predictions of HHT NNLO (top) and HERAPDF2.0 NNLO (bottom), both with $Q^2_{\text{min}} = 3.5\,\text{GeV}^2$, compared to the HERA measurements of σ_r. The bands represent the experimental, i.e. fit, uncertainties. Extrapolations are indicated as dotted lines.

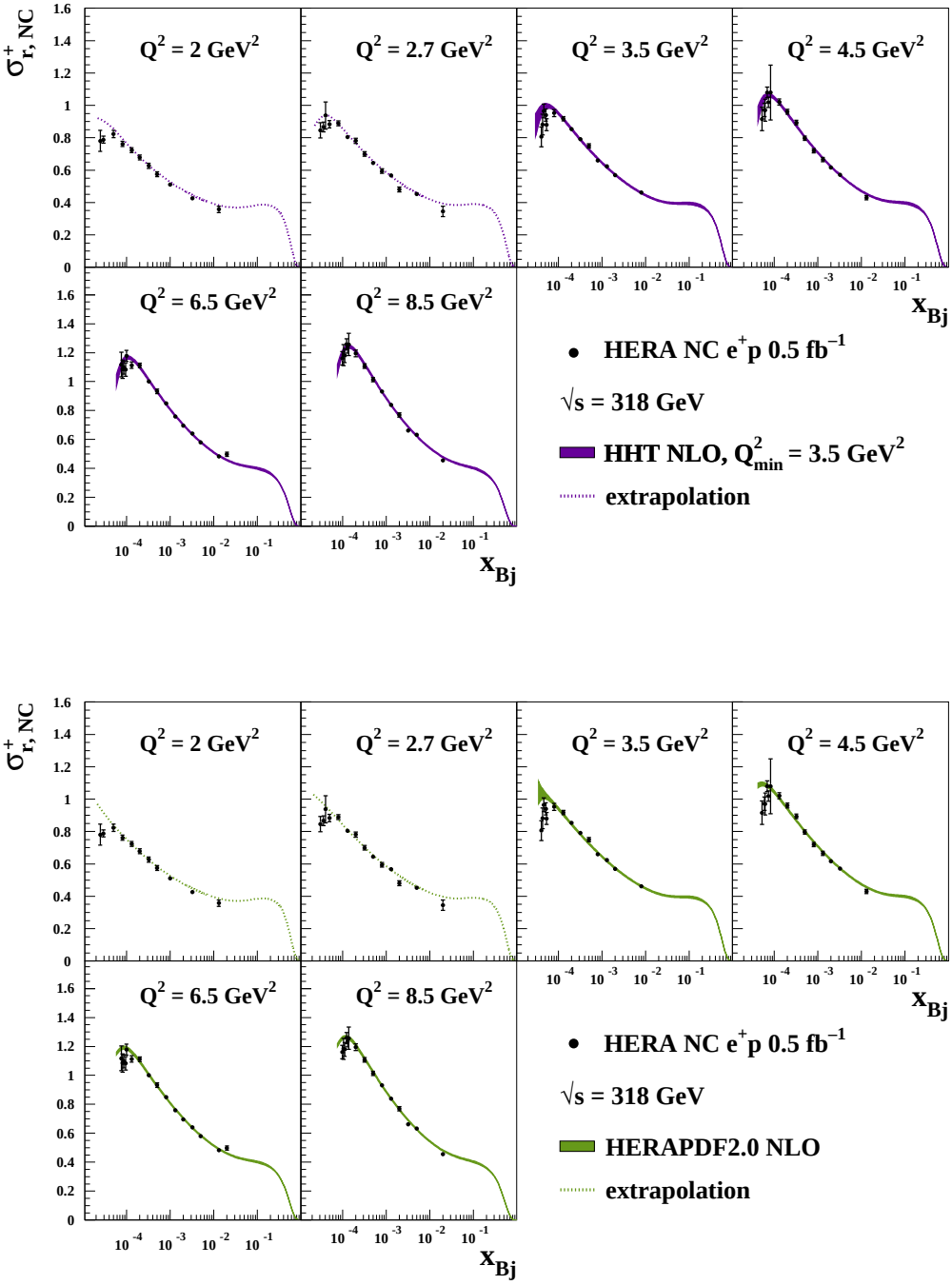

Figure 5: The predictions of HHT NLO (top) and HERAPDF2.0 NLO (bottom), both with $Q^2_{\text{min}} = 3.5\,\text{GeV}^2$, compared to the HERA measurements of σ_r. The bands represent the experimental, i.e. fit, uncertainties. Extrapolations are indicated as dotted lines.

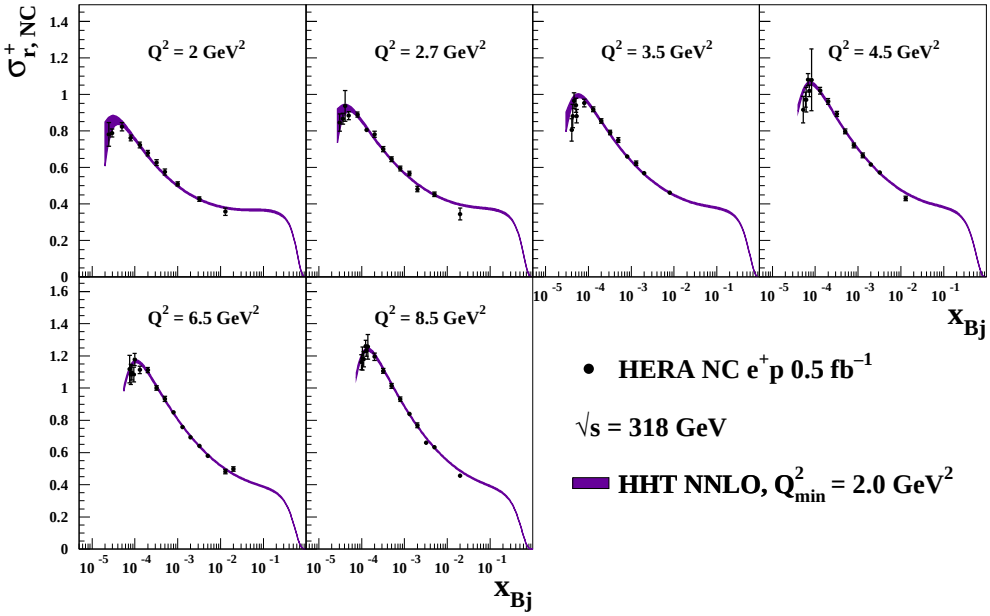

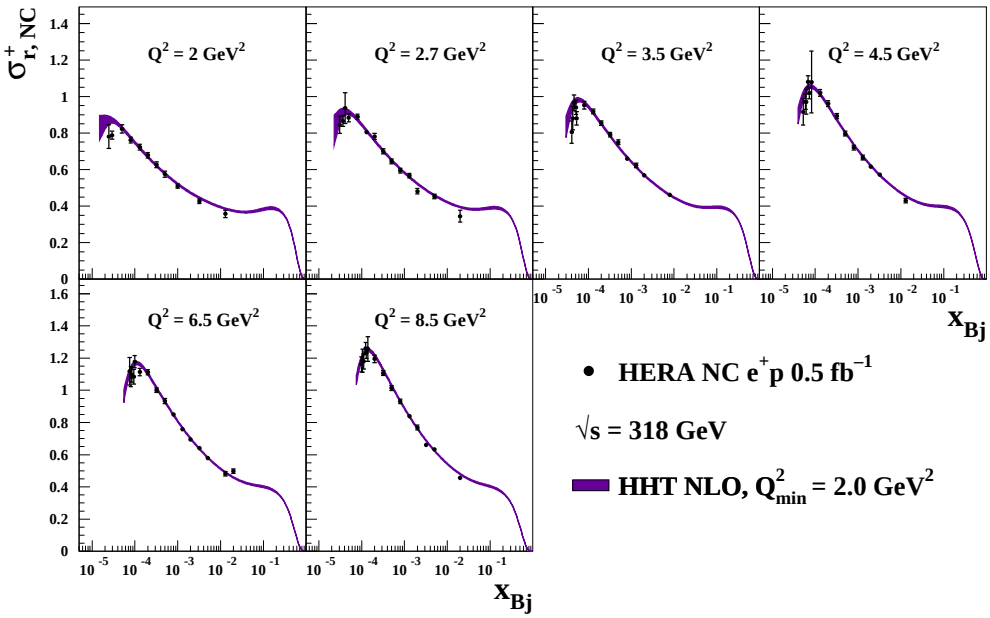

Figure 6: The predictions of HHT NNLO (top) and HHT NLO (bottom) with $Q^2_{\rm min} = 2.0\,{\rm GeV}^2$ compared to the HERA measurements of σ_r. The bands represent the experimental, i.e. fit, uncertainties.

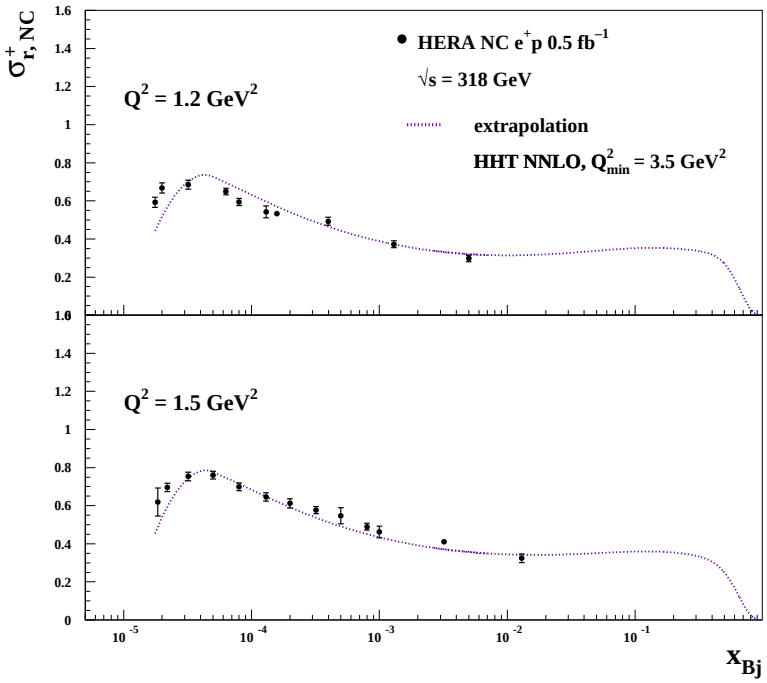

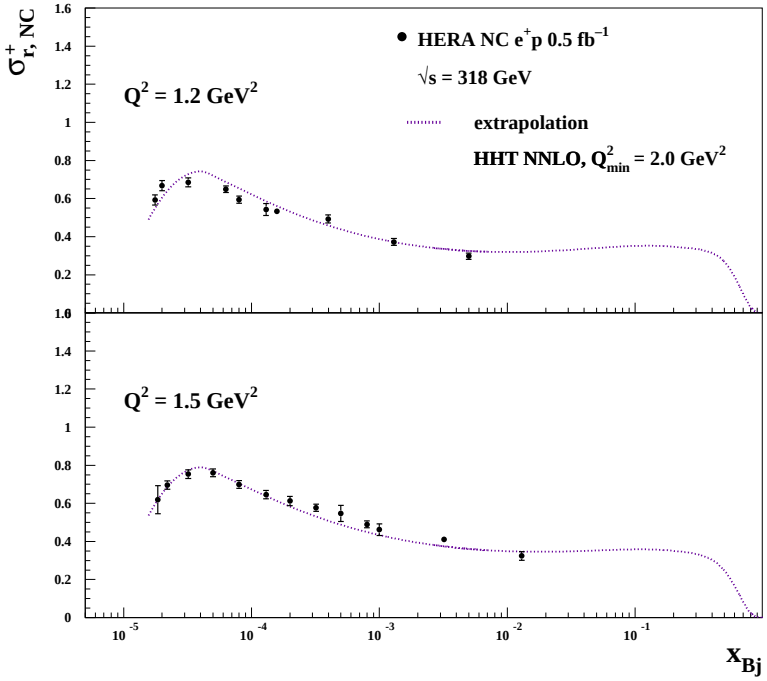

Figure 7: The extrapolated predictions of HHT NNLO with with $Q^2_{\rm min} = 3.5\,{\rm GeV}^2$ (top) and with $Q^2_{\rm min} = 2.0\,{\rm GeV}^2$ (bottom) compared to the HERA NC e^+p measurements of σ_r at Q^2 of 1.2 and $1.5\,{\rm GeV}^2$.

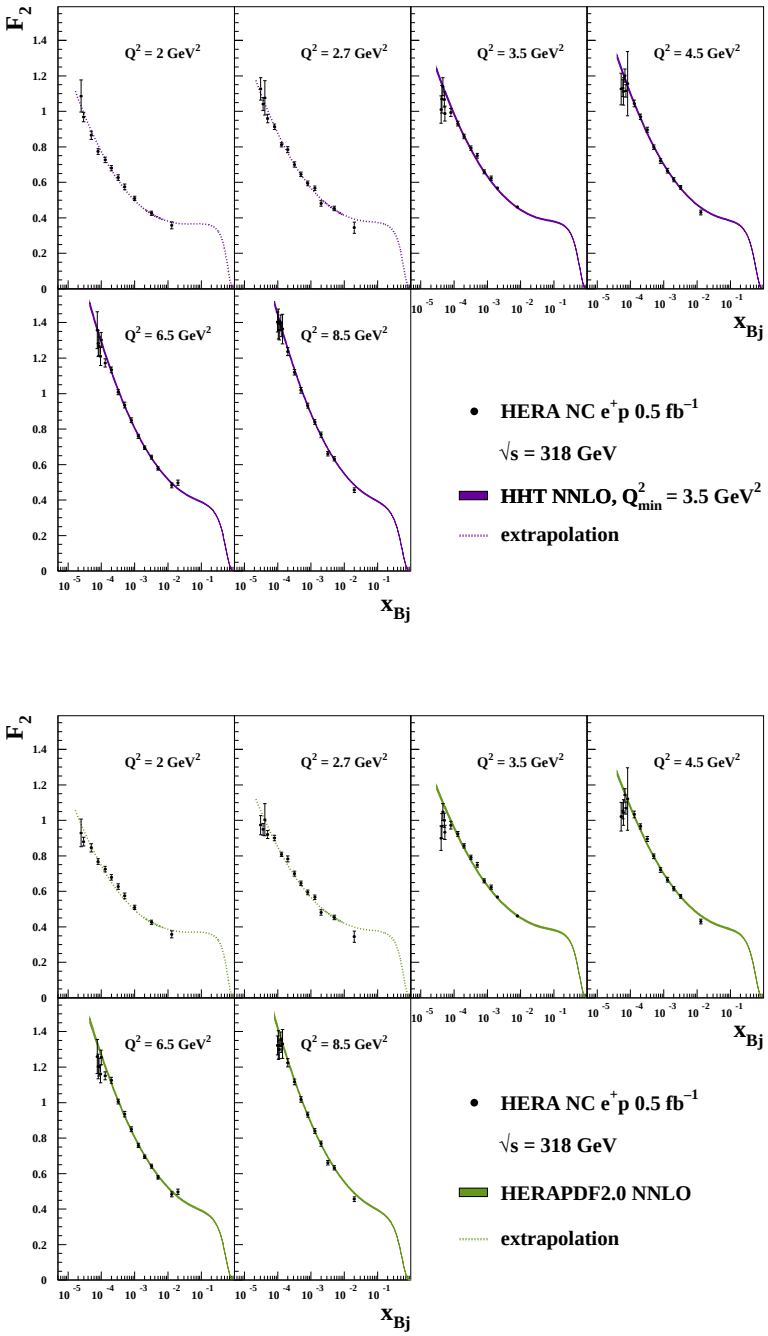

Figure 8: The predictions of HHT NNLO (top) and HERAPDF2.0 NNLO (bottom), both with $Q^2_{\text{min}} = 3.5\,\text{GeV}^2$, compared to extracted values $F_2^{\text{extracted}}$. The bands represent the experimental, i.e. fit, uncertainties. Extrapolations are indicated as dotted lines.

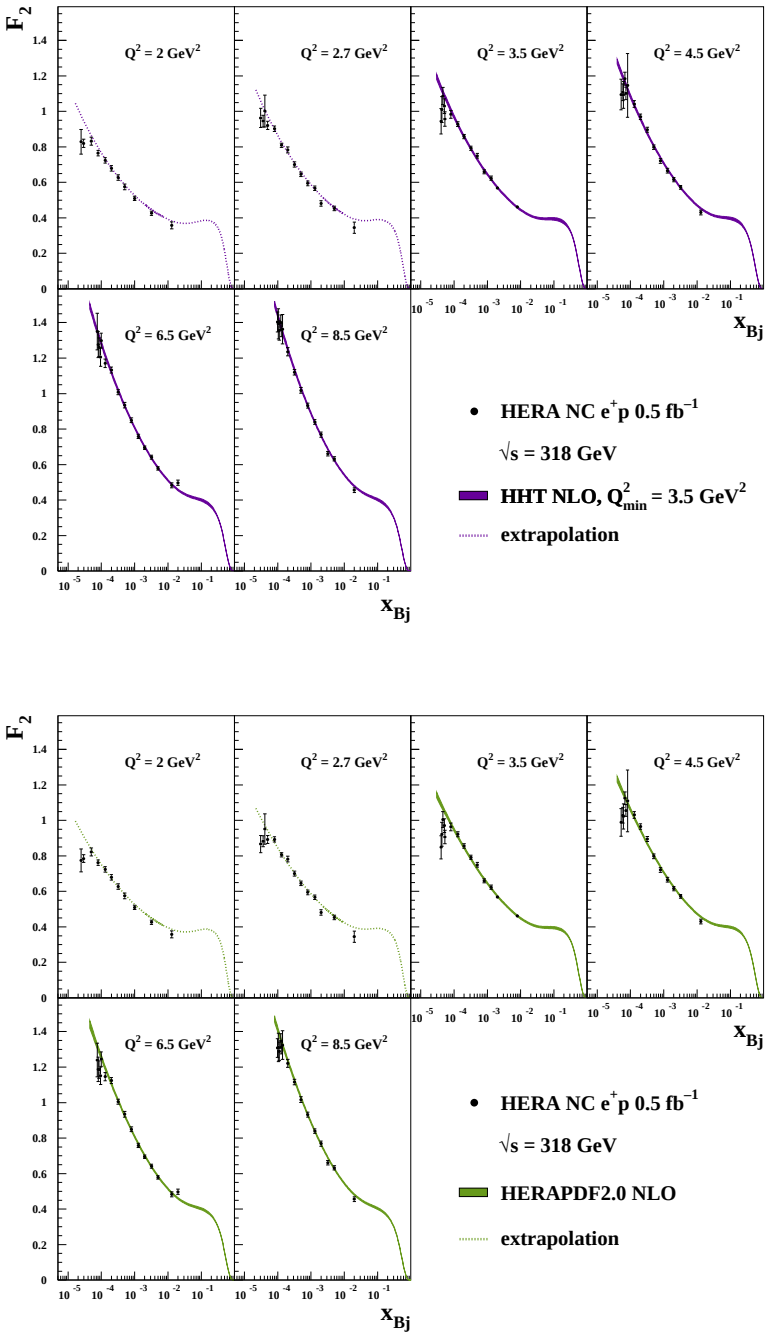

Figure 9: The predictions of HHT NLO (top) and HERAPDF2.0 NLO (bottom) both with $Q^2_{\text{min}} = 3.5\,\text{GeV}^2$, compared to extracted values $F_2^{\text{extracted}}$. The bands represent the experimental, i.e. fit, uncertainties. Extrapolations are indicated as dotted lines.

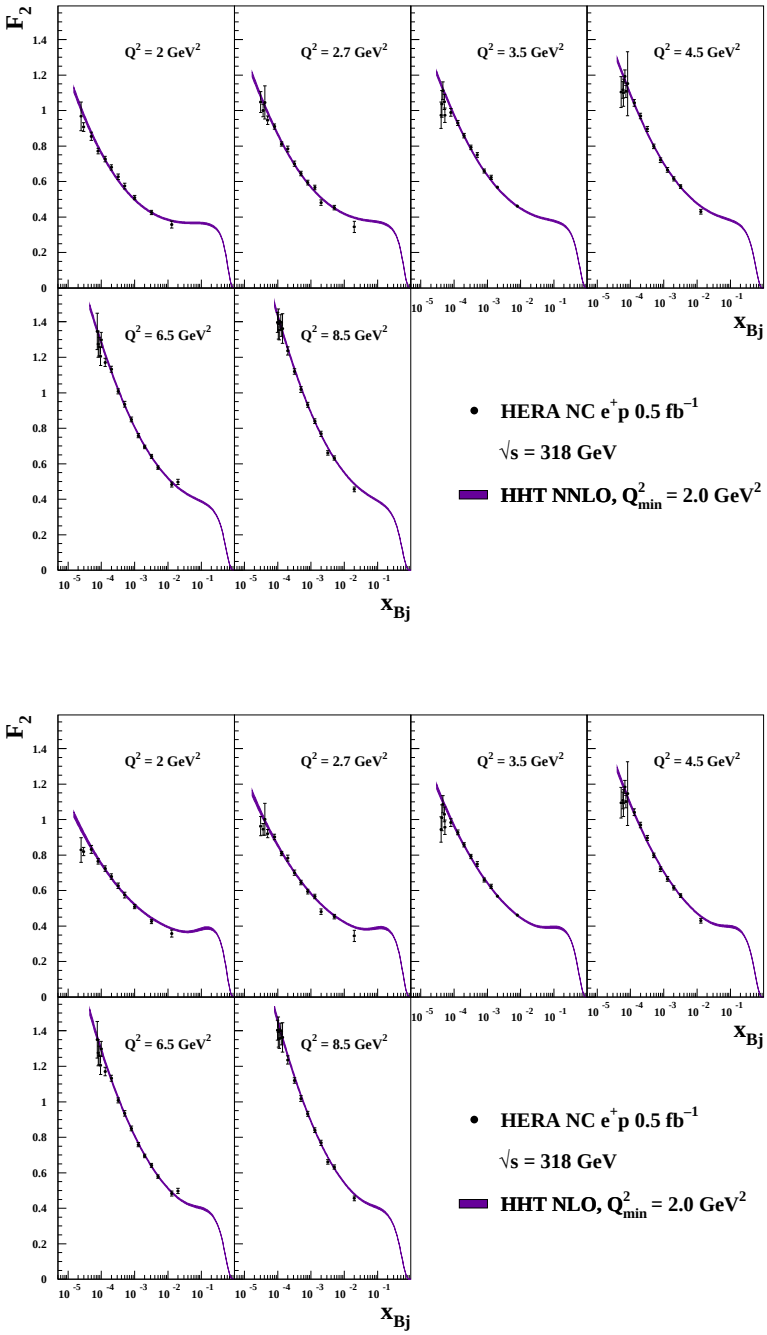

Figure 10: The predictions of HHT NNLO (top) and HHT NLO (bottom) with $Q^2_{\text{min}} = 2.0\,\text{GeV}^2$ compared to extracted values $F_2^{\text{extracted}}$. The bands represent the experimental, i.e. fit, uncertainties.

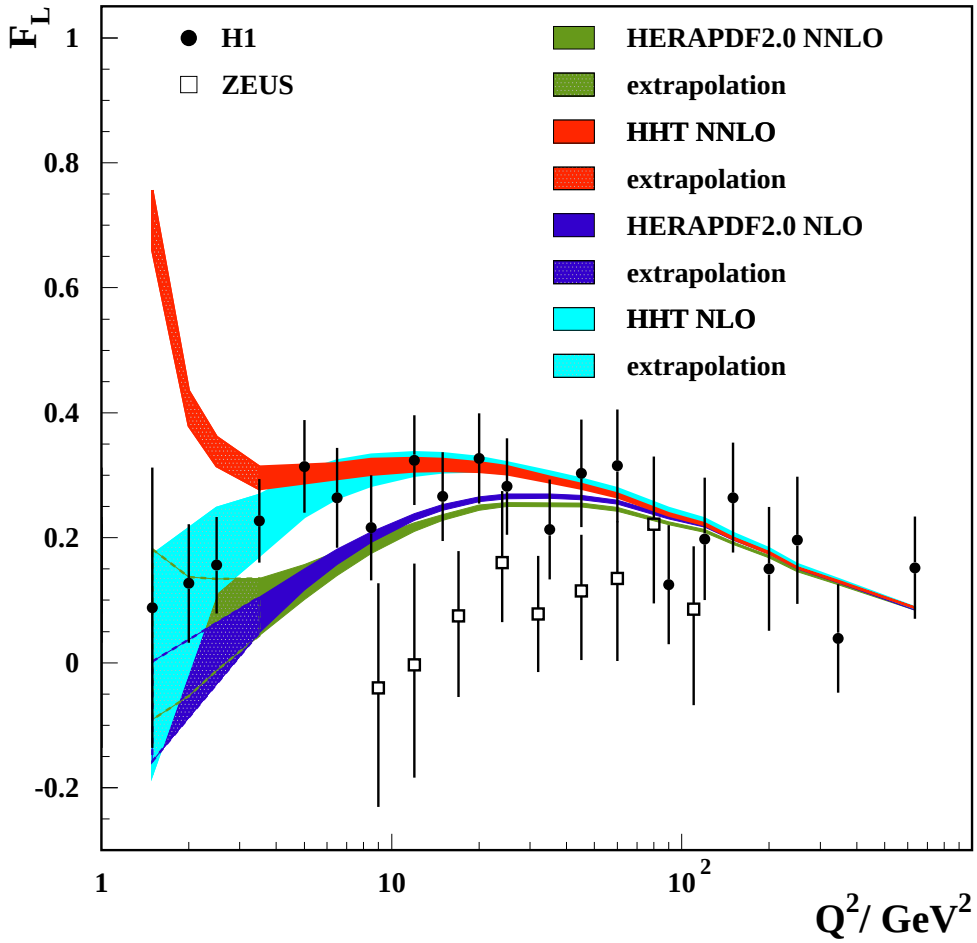

Figure 11: The predictions for F_{L} from HHT and HERAPDF2.0, both with $Q^2_{\mathrm{min}} = 3.5\,\mathrm{GeV}^2$, compared to the separate direct measurements published by the H1 and ZEUS collaborations. The bands represent the experimental, i.e. fit, uncertainties on the predictions. Hatched bands represent extrapolations.

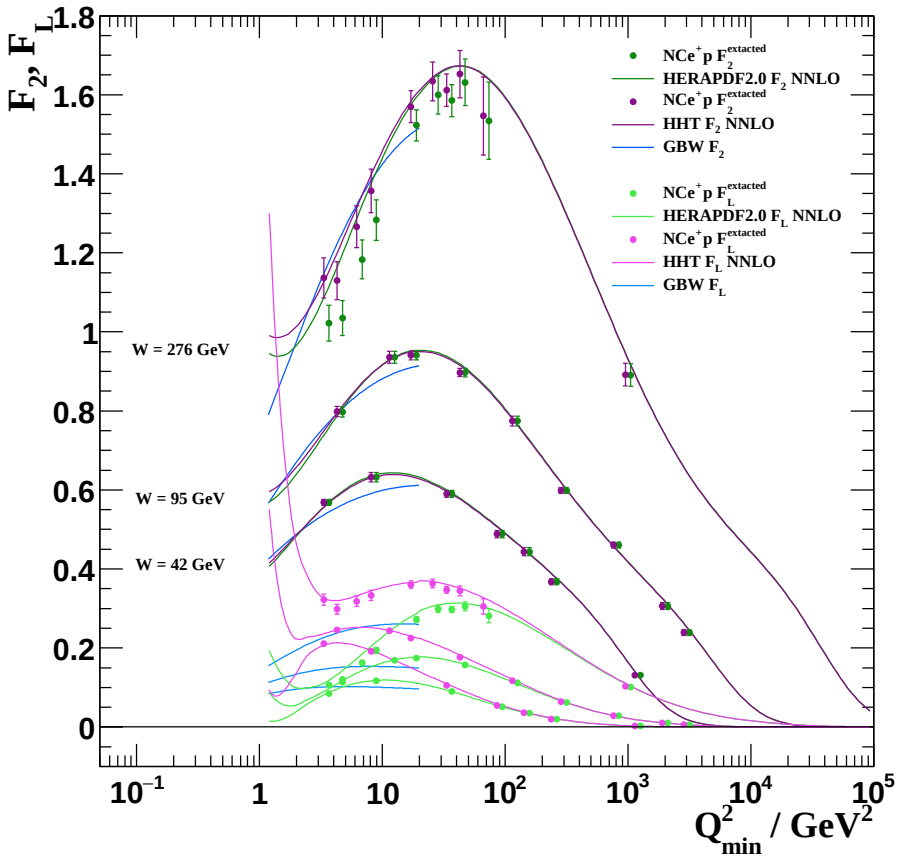

Figure 12: The $F_2^{\text{extracted}}$ and $F_L^{\text{extracted}}$ values as extracted from HHT NNLO and HERAPDF2.0 NNLO together with the corresponding predictions from HHT NNLO and HERAPDF2.0 NNLO for three selected values of W. Also shown are predictions from the GBW model.

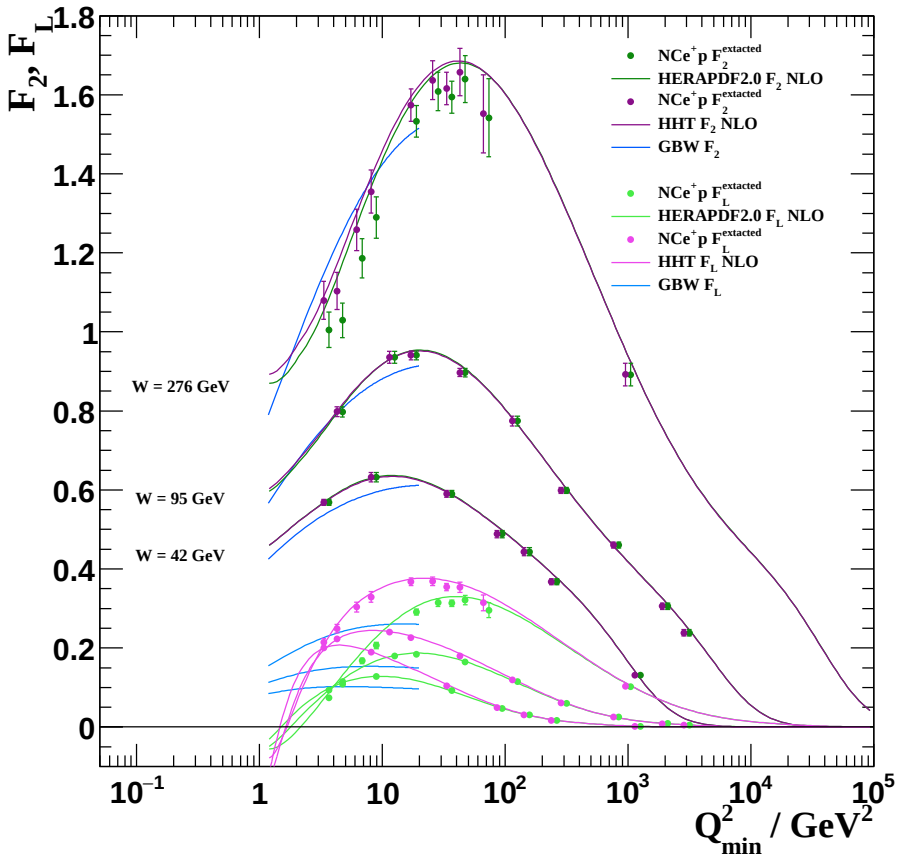

Figure 13: The $F_2^{\text{extracted}}$ and $F_L^{\text{extracted}}$ values as extracted from HHT NLO and HERAPDF2.0 NLO together with the corresponding predictions from HHT NLO and HERAPDF2.0 NLO for three selected values of W. Also shown are predictions from the GBW model.

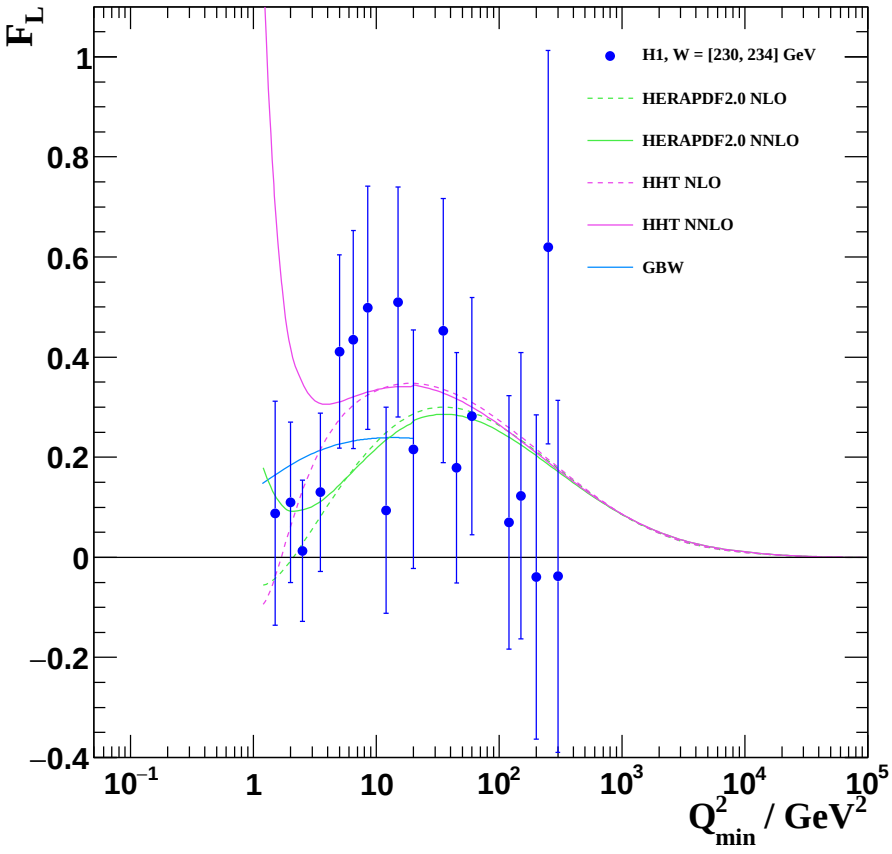

Figure 14: The predictions from HHT and HERAPDF2.0 at NNLO and NLO for $W = 232$ GeV, together with direct measurements of F_L published by the H1 collaboration for W between 230 and 234 GeV. Also shown is the prediction from the GBW model.